Compensation of airflow maldistribution in fin-and-tube evaporators

Kærn, Martin Ryhl; Tiedemann, Thomas

Published in:
Proceedings of the 14th International Refrigeration and Air Conditioning Conference

Publication date:
2012

Compensation of airflow maldistribution in fin-and-tube evaporators

Martin Ryhl Kærn[1]*, Thomas Tiedemann[2]

[1]Technical University of Denmark, Department of Mechanical Engineering,
Kongens Lyngby, Denmark,
Tel: +45 4525 4121, Fax: +45 4593 5215, Email: pmak@mek.dtu.dk

[2]Danfoss GmbH, Refrigeration and Air-Conditioning
Offenbach, Germany
Tel.: +49 69 47868 550, Fax: +49 69 8902 466 843, Email: Thomas.Tiedemann@danfoss.com

* Corresponding Author

ABSTRACT

Compensation of airflow maldistribution in fin-and tube evaporators for residential air-conditioning is investigated with regards to circuitry design and control of individual channel superheats. In particularly, the interlaced and the face split circuitry designs are compared numerically using a linear velocity profile and a CFD predicted velocity profile obtained from Kærn (2011d) in dry and wet conditions. The circuitry models are validated experimentally in wet conditions, and for this purpose a test case interlaced evaporator (17.58 kW) was reconstructed in order to become a face split evaporator by modifying its U-bend connections. Furthermore, a 14% and 28% blockage of the face split evaporator is studied experimentally with control of individual channel superheats. It is shown that the face split circuitry with compensation gives the best performance in both dry and wet conditions, however with lower gains in wet conditions (around 3% in cooling capacity and 7-9% in UA-value). This performance gain in cooling capacity is below the uncertainty in standard experiments, however the gain may be revealed and/or validated by the possible area savings experimentally, i.e. in terms of overall UA-value.

1. INTRODUCTION

For A-shaped fin-and-tube evaporators employed in residential air-conditioning, the chosen type changed a couple of years ago by manufacturers. It changed from the face split to the interlaced circuitry, see Figure 1. The interlaced circuitry shows a significant increase in cooling capacity compared to the face split circuitry. The main reason is the better compensation of flow maldistribution by design. In the current paper this choice is discussed with regards to further compensation of flow maldistribution by control of individual channel superheats.

Flow maldistribution in fin-and-tube evaporators has been shown to decrease the performance of the evaporator and the system both experimentally (Payne and Domanski, 2003) and numerically (Kærn *et al.*, 2011a, Kim *et al.*, 2009b). Both air side and refrigerant side effects may cause flow non-uniformities, e.g. non-uniform airflow, air-temperature, humidity or frost, fouling, two-phase inlet distribution, feeder tube bending and improper heat exchanger design. In this study we only address a non-uniform airflow to the evaporator.

Most efforts of compensating flow maldistribution have been addressed to the design of the evaporator circuitry. Domanski and Yashar (2007) applied a novel optimization system called ISHED (intelligent system for heat exchanger design) to optimize refrigerant circuitry in order to compensate airflow maldistribution. They measured the air velocity profile using particle image velocimetry (PIV) and used that as input to their numerical model and reported that the cooling capacity was increased by 4.2% compared to an interlaced type of circuitry.

Studies regarding the benefits by control of individual superheat have also been conducted. Payne and Domanski (2003) showed experimentally that the performance degradation due to a non-uniform airflow could be recovered to within 2% of the original cooling capacity at uniform airflow conditions. Kim *et al*. (2009a) studied benefits of upstream vs. downstream control of individual channel superheat on a fin-and-tube five channel R410A heat pump numerically. The study showed that the upstream control outperformed the downstream control. They found that upstream control was able to recover up to 99.9% of the penalties of maldistribution. Kærn *et al*. (2011b) also studied compensation by control of individual channel superheat. Here a recovery of 94.3% in COP was found at a nearly complete air blockage of half of the evaporator, keeping the total air volume flow constant.

Recently, Kærn *et al*. (2011c) studied the combination of tube circuitry (face split and interlaced) and control of individual channel superheat on an 8.8 kW R410A A-coil evaporator in dry air conditions. It was shown that the interlaced evaporator is better at flow maldistribution than the face split evaporator. However, if the individual channel superheats were controlled, the face split evaporator achieved the best performance, i.e. an increase of 7% in UA-value and 1.6% to 2.4% in COP compared to the interlaced evaporator without compensation.

The objective of this paper is to study and validate the hypothesis from Kærn *et al*. (2011c), i.e. that the face split evaporator performs better in terms of cooling capacity and UA-value than the interlaced evaporator with control of individual channel superheats. For this purpose an experimental test case interlaced evaporator (17.58 kW) was reconstructed in order to become a face split evaporator by modifying its U-bend connections. Apart from earlier numerical studies in Kærn *et al*. (2011c), we have in this study considered a larger evaporator with three tube rows, introduced a model for dehumidifying conditions, and introduced a CFD predicted airflow profile, which serves as a better velocity profile guess than a linear profile. The method of compensation involves a coupled expansion and distributor device marketed as EcoFlow(TM), which is able to distribute the mass flow according to the individual superheat of each channel by only measuring the overall superheat (Funder-Kristensen *et al*., 2009; Mader and Thybo, 2010).

The paper includes a brief description of the numerical model, an analysis of airflow maldistribution in both evaporators (dry and wet conditions), and compensation by control of individual channel superheat. Furthermore, a 14% and 28% blockage of the face split evaporator is studied experimentally with control of individual channel superheats.

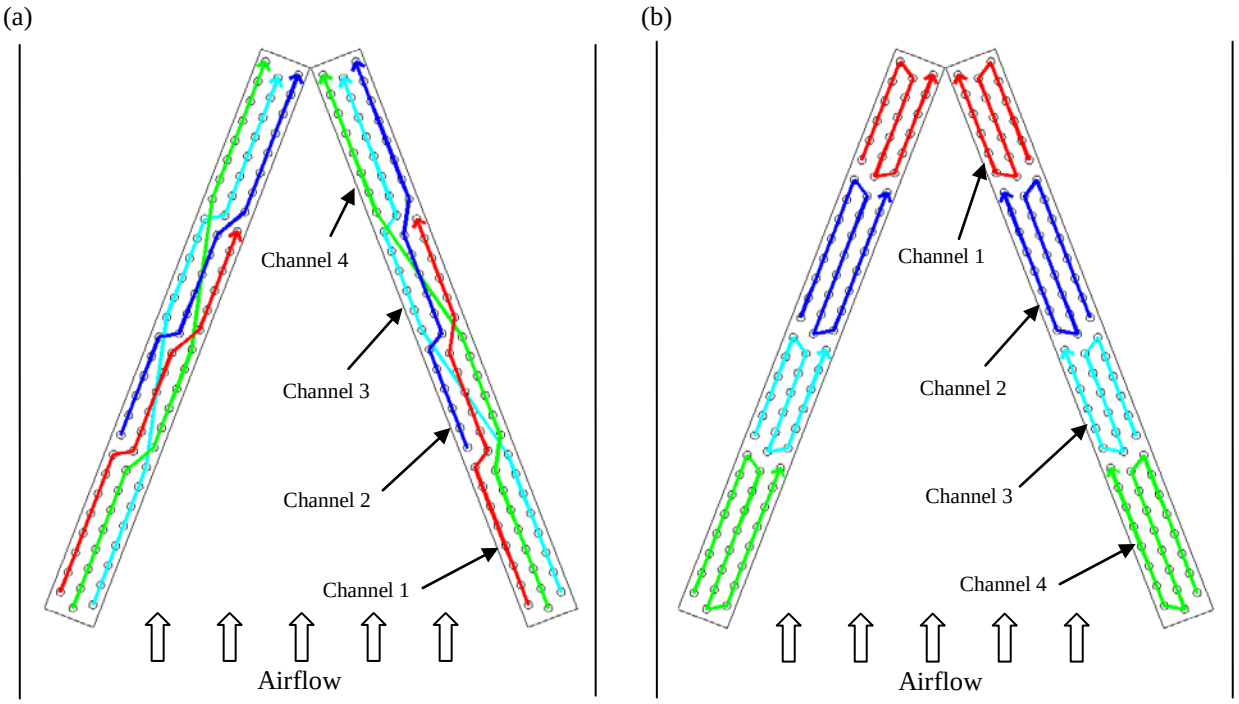

Figure 1: Tube circuitries of (a) the interlaced evaporator and (b) the face split evaporator

2. SIMULATION MODEL

A model of an 8.8 kW R410A evaporator was developed by Kærn *et al*. (2011a) in Dymola 7.4, and it has been updated in this study to include the tube circuiting effects of the 17.58 kW evaporator and dehumidifying conditions. Thermophysical properties for R410A are obtained from the refeqns package (Skovrup, 2009). In order to predict the refrigerant maldistribution in the evaporator a distributed one-dimensional mixture model was chosen that computes local heat transfer and pressure drop (evaporator tubes, feeder tubes and bends).

2.1 Geometry and correlations

The evaporator consists of two coils each with 4 refrigerant channels. There are 28 tubes per tube row and 3 tube rows as shown in Figure 1. The tube length is 444.5 mm. The tube inner and outer diameter is 8.52 mm and 9.52 mm, respectively. The transverse and longitudinal tube pitch is 25.4 mm and 21.25 mm, respectively. The fins are louvered and the fin pitch is 2.12 mm. The total outside surface area is 35.0 m2. The tube inner walls are smooth. Furthermore, the feeder tubes to the evaporator have an internal diameter of 4.95 mm and a length of 300 mm. Note that the coil geometry is the same for both the interlaced and face split evaporator, however the tube connections or circuiting are different as shown on Figure 1. The two coils in the evaporator are assumed to be in similar maldistribution conditions and thus perform similarly despite the small circuitry differences in the two interlaced coils (the right hand side coils in Figure 1a and 1b were simulated).

We choose to use 3 discrete cells per tube equalling 252 cells plus 80 adiabatic U-bend cells. Each cell of the evaporator is calculated as a small heat exchanger with uniform transport properties. Mass, momentum and energy conservation equations are applied to the refrigerant in each cell, where homogeneous flow and thermodynamic equilibrium are assumed. Furthermore, changes in kinetic and potential energies are neglected. It is assumed that the tube walls have rotational symmetry, i.e. no heat conduction in the azimuthal direction. The used correlations for both the evaporator and the condenser are given in table 1. Furthermore, effectiveness-NTU relations for cross flow heat exchangers are employed. Dehumidifying conditions are computed similarly to Jiang (2003), where the Colburn analogy is used and the assumption of a linear dehumidifying process path, i.e. a linear relationship between the temperature and humidity ratio difference. It enables the use of the temperature difference as driving potential for the combined heat and mass transfer problem such that both fin efficiency and effectiveness-NTU relations for dry air also can be used for dehumidifying conditions. A discrete cell is in dehumidifying conditions if the mean fin surface temperature is below the dew point temperature of the air.

Table 1: Overview of used correlations

Air-side	Heat transfer	Wang *et al*. (1999)
	Fin efficiency	Schmidt (1949), (Schmidt approximation)
Single phase	Heat transfer	Gnielinski (1976)
	Friction	Blasius
	Bend friction	Ito (1960)
Two-phase	Heat transfer	Shah (1982)
	Friction	Müller-Steinhagen and Heck (1986)
	Bend friction	Geary (1975)

2.2 Airflow distribution

In this study we have applied both a CFD predicted airflow profile and a linear velocity profile. The linear velocity profile is constructed by using the airflow distribution parameter, F_{air}, which is defined by

$$V(y) = V_m F_{air} + y\frac{2V_m(1-F_{air})}{L_t} \quad (1)$$

Where V_m = mean frontal velocity [m/s], y = transverse coordinate [m], L_t = transverse length of the coil [m]. When F_{air} is unity, the airflow profile is uniform across the coil, see Figure 2a. When F_{air} is zero, the airflow profile becomes the worst possible linear one-dimensional profile in the transverse direction, see Figure 2b. Furthermore, Figure 2c shows the CFD predicted airflow profile. The CFD prediction is obtained using commercial CFD code

STAR-CD (2005) and extrapolated to actual evaporator size and airflow rate. More information on grid and solution procedure is given in Kærn (2011d). The prediction showed a recirculation zone in the bottom of the coils, which cannot be handled by the current numerical model, i.e. have negative perpendicular velocities locally. For these reasons, the airflow profile was corrected such that no air flows through the recirculation zone in the bottom of the coil (as indicated on Figure 2c), while keeping the overall air volume flow constant.

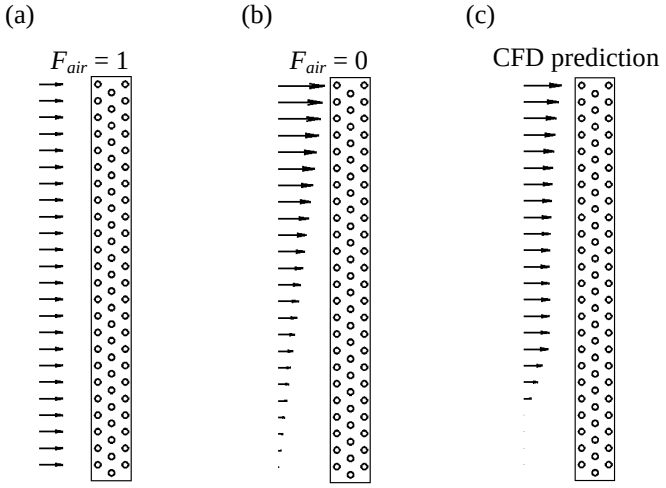

Figure 2: Applied one-dimensional airflow profile

2.3 Boundary conditions

The boundary conditions on the refrigerant side are an overall superheat of 5 K, a volume outflow of 11.3 m^3/hr and a liquid temperature before expansion of 46°C. The total air volume flow rate is 0.85 m^3/s (avg. frontal velocity of 1.35 m/s) and the air temperature is 26.7°C. In wet conditions the wet bulb temperature is 19.4°C. When compensating, the expansion device controls each channel superheats to 5 K.

2.4 Experimental validation

The numerical model of the evaporator is validated in wet conditions for both the interlaced and face split circuitries as shown on Figure 1 with experiments carried out at Danfoss A/S Nordborg. The experiments are directly comparable and performed at similar indoor and outdoor conditions, however, the evaporator boundary conditions became slightly different because of the two different circuitries (for example volume outflow and liquid temperature differs slightly), thus the numerical results cannot directly be compared, but should instead be compared to each experiment. Furthermore, we used the CFD profile from Figure 2c in the model. In addition, we used compensation by control of individual channel superheats in these comparisons. Table 2 shows the comparison between the experiments and the model results.

The uncertainty of the capacity measure is 5% and the experiments show that the energy balance agrees within 3%. With this uncertainty in the experiments it is difficult to claim which evaporator performs best, however, the numerical results agrees well with the experimental data and thus we may use the numerical model to analyze the circuitry effects in more detail.

Table 2: Validation

	Interlaced		Face split	
	Experiment	Model	Experiment	Model
Cooling capacity (air-side)	16.04 kW	15.46 kW	15.56 kW	15.55 kW
Cooling capacity (ref-side)	15.67 kW	15.46 kW	16.01 kW	15.55 kW
Mass flow rate	0.0931 kg/s	0.0918 kg/s	0.0955 kg/s	0.0929 kg/s
Evaporator outlet pressure	10.53 bar	10.39 bar	10.73 bar	10.46 bar
Sensible heat	12.57 kW	12.68 kW	12.27 kW	12.93 kW
Latent heat	3.41 kW	2.78 kW	3.24 kW	2.62 kW

3. RESULTS

In this section the results of the simulations of airflow maldistribution are presented for each circuitry type in dry and wet conditions with and without compensation by control of individual channel superheat. The airflow distribution parameter is varied individually from 1 to 0, imposing an increasing degree of linear airflow maldistribution. In addition, the CFD predicted airflow profile is simulated.

3.1 Comparison of the interlaced and face split evaporators in dry conditions (linear profile)

Figure 3 shows the cooling capacity and overall UA-value as function of the air distribution parameter in dry conditions. The Figure also shows the normalized results by the system that is mostly used today, i.e. the interlaced evaporator without compensation (EXV) so that the actual percentage increase or decrease can be viewed by using another system. The results show that the interlaced circuitry performs better than the face split circuitry without compensation at both uniform conditions and increasing airflow maldistribution (full lines). This result is in contrast to the result in Kærn (2011c), where the face split evaporator performed better in uniform conditions, however, the consequence of the current face split having unequal number of tubes in each channel. Referring to Figure 1, channel 1 and 3 have only 18 tubes and channel 2 and 4 have 24 tubes. The result is that liquid comes out of channel 1 and 3 of the face split evaporator at uniform conditions. Furthermore, the decrease in performance by the interlaced evaporator without compensation as F_{air} goes towards zero is lower than for the face split evaporator. It shows that the interlaced evaporator compensates the airflow maldistribution better by design.

When using the compensation method the face split evaporator performs the best at all values of F_{air}. This result is similar to the result in Kærn (2011c) and is because of the tube circuitry. The channels in the face split evaporator are counter-cross flow, however the interlaced is a mix of both counter-cross flow and parallel-cross flow. When constructing a heat exchanger it should always be attempted to use the temperature potential between the heat exchanging fluids in the best possible way. It is not the case when the superheated regions, which have lower UA-value, are aligned next to each other in the flow direction, as for the interlaced evaporator. There is a higher temperature potential for heat transfer in all superheated regions of the face split evaporator, since they are aligned

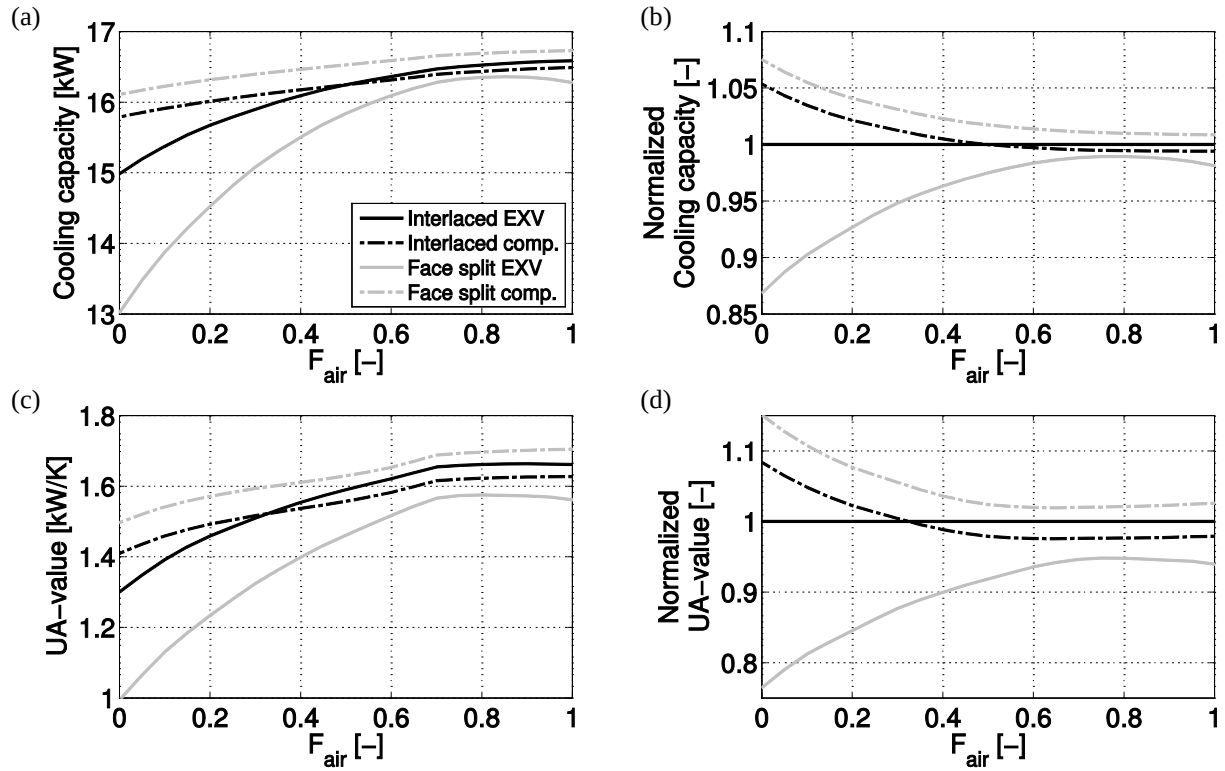

Figure 3: Cooling capacity and overall UA-value vs. the air distribution parameter (dry conditions)

in the first tube row. In turn, the face split evaporator will minimize the superheated region, since the gradient of the refrigerant vapor is higher than for the interlaced evaporator. Interestingly, the interlaced evaporator without compensation performs better than the interlaced with compensation. This is because channel 1 and 2 with outlets in the back tube row has the lowest superheat while the superheats of channel 3 and 4 are higher in the front of the coil. Controlling channel 1 and 2 to increase their superheat to equal the overall superheat will increase the overall superheated area, and thus decrease performance. Therefore, it is not always optimal to have equal channel superheats. This effect is however only at $F_{air} > 0.5$ and for the interlaced evaporator.

By using the compensation method on the face split evaporator in dry conditions shows that the cooling capacity and overall UA-value increase may become as much as 7.5% and 15%, respectively.

3.2 Comparison of the interlaced and face split evaporators in wet conditions (linear profile)

Figure 4 shows the cooling capacity and overall UA-value as function of the air distribution parameter in wet conditions. Again the Figure shows the normalized results by the system that is mostly used today, i.e. the interlaced evaporator without compensation (EXV). In addition, the sensible and latent heat loads are shown. Note

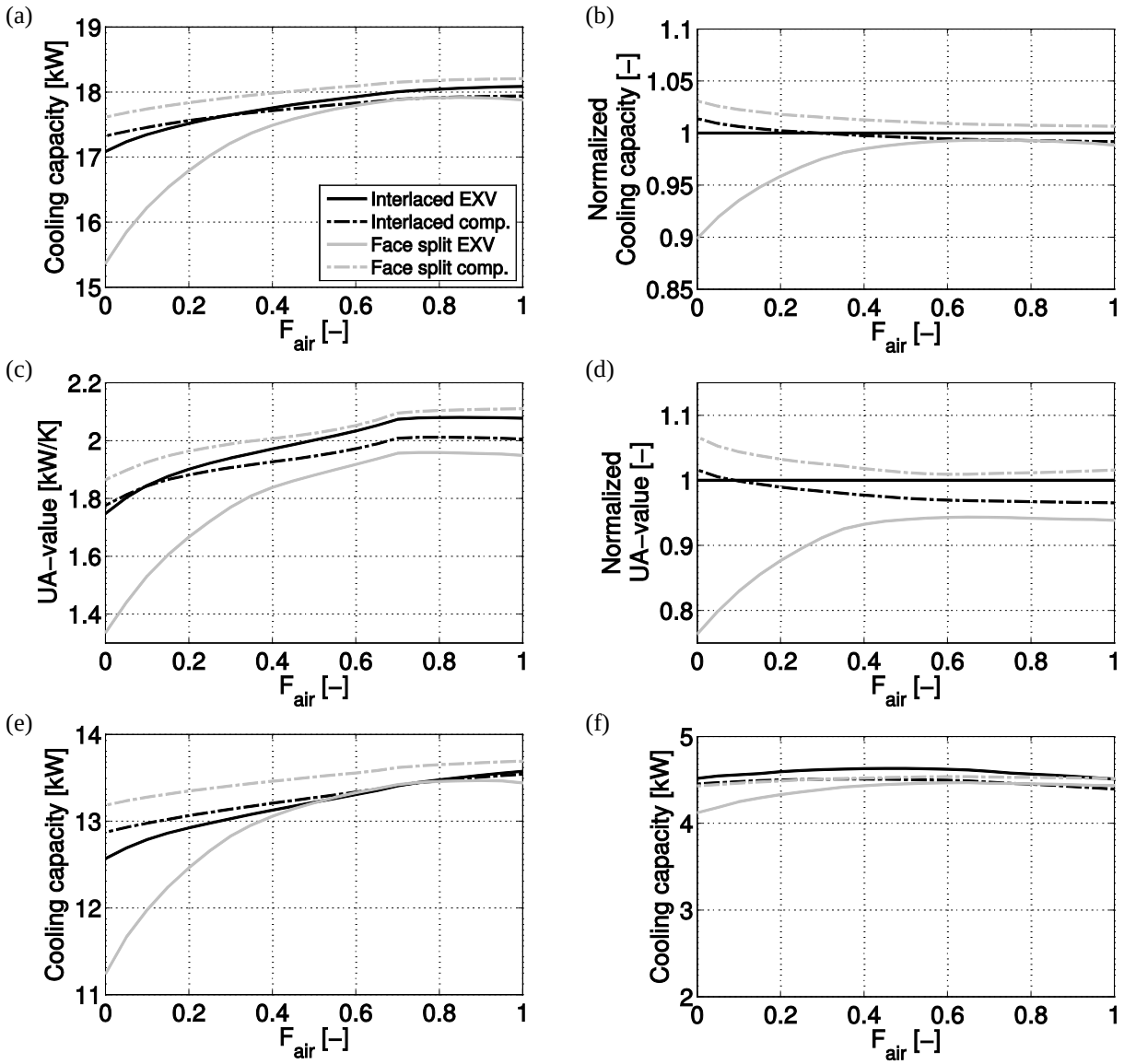

Figure 4: Cooling capacity and overall UA-value vs. the air distribution parameter (wet conditions)

that the overall UA-value here takes into account the combined heat and mass transfer on the air side. (incl. water vapor condensation).

The results show basically the same trends as in dry conditions in terms of cooling capacity and overall UA-value, however, the performance improvements using the compensation method on the face split evaporator is reduced. The reason is because of the better heat transfer on the air-side in wet conditions that will raise the wall and refrigerant evaporation temperature, thus reducing the temperature difference to the air flowing through the evaporator. In other words, the face split evaporator does not gain as much by having the superheated region in the front tube row, where the temperature driving potential is highest. For the interlaced evaporator the results show that only at large degrees of airflow maldistribution is it beneficial to use the compensation method. Looking into the details of the sensible and latent heat loads (Figure 4e and 4f), reveals that the sensible results are similar to the results obtained in dry conditions, however, the latent results show that the interlaced without compensation gives the highest heat load. This is because of a lower superheat in the back tube row that results in more water vapor condensation.

Using the compensation method on a face split evaporator in wet conditions shows that the cooling capacity and overall UA-value increase may become as much as 3.1% and 6.7%, respectively.

3.3 Comparison of the interlaced and face split evaporators using the CFD predicted air profile

Table 3 shows the results of using the CFD predicted air profile in dry and wet conditions. The CFD profile serves as a better guess of the airflow profile across the coils, which was validated in section 2.4. Again the results show that the face split evaporator performs the best with compensation by control of individual channel superheat and that the performance gains reduce in wet conditions. The interlaced evaporator with compensation also performs better in both dry and wet conditions compared to the interlaced without compensation. This means that the air distribution parameter, F_{air}, with similar performance is close to zero (compared to Figure 4).

Table 3: Cooling capacity (Q_e) and overall UA-value using the CFD predicted air profile

	Dry conditions				Wet conditions			
	Q_e [kW]	Q_e [%] change	UA [kW/K]	UA [%] change	Q_e [kW]	Q_e [%] change	UA [kW/K]	UA [%] change
Face split comp.	16.25	+5.8	1.483	+14.60	17.66	+2.8	1.816	+9.10
Interlaced comp.	15.98	+4.1	1.395	+7.8	17.39	+1.3	1.707	+2.56
Face split EXV	12.82	-16.5	0.898	-30.7	14.75	-14.1	1.132	-32.0
Interlaced EXV	15.35	0	1.294	0	17.16	0	1.665	0

Figure 5 shows the refrigerant temperature contours and outlet superheats. It is seen that the compensation method reduces the total superheated zone in both the face split and interlaced evaporator, however much more significant for the face split evaporator. This is because of the tube circuitry where the interlaced evaporator compensates the airflow maldistribution to some extent by design. Interestingly, liquid comes out of channel 1 in the interlaced evaporator without compensation, which is the reason why the latent heat is higher for the interlaced evaporator without compensation in Figure 4f. It will cause a lower wall temperature and more water vapor condensation, in contrast to with compensating. Furthermore, it is seen that the evaporating temperatures are increased in wet conditions, which reduces the performance gains.

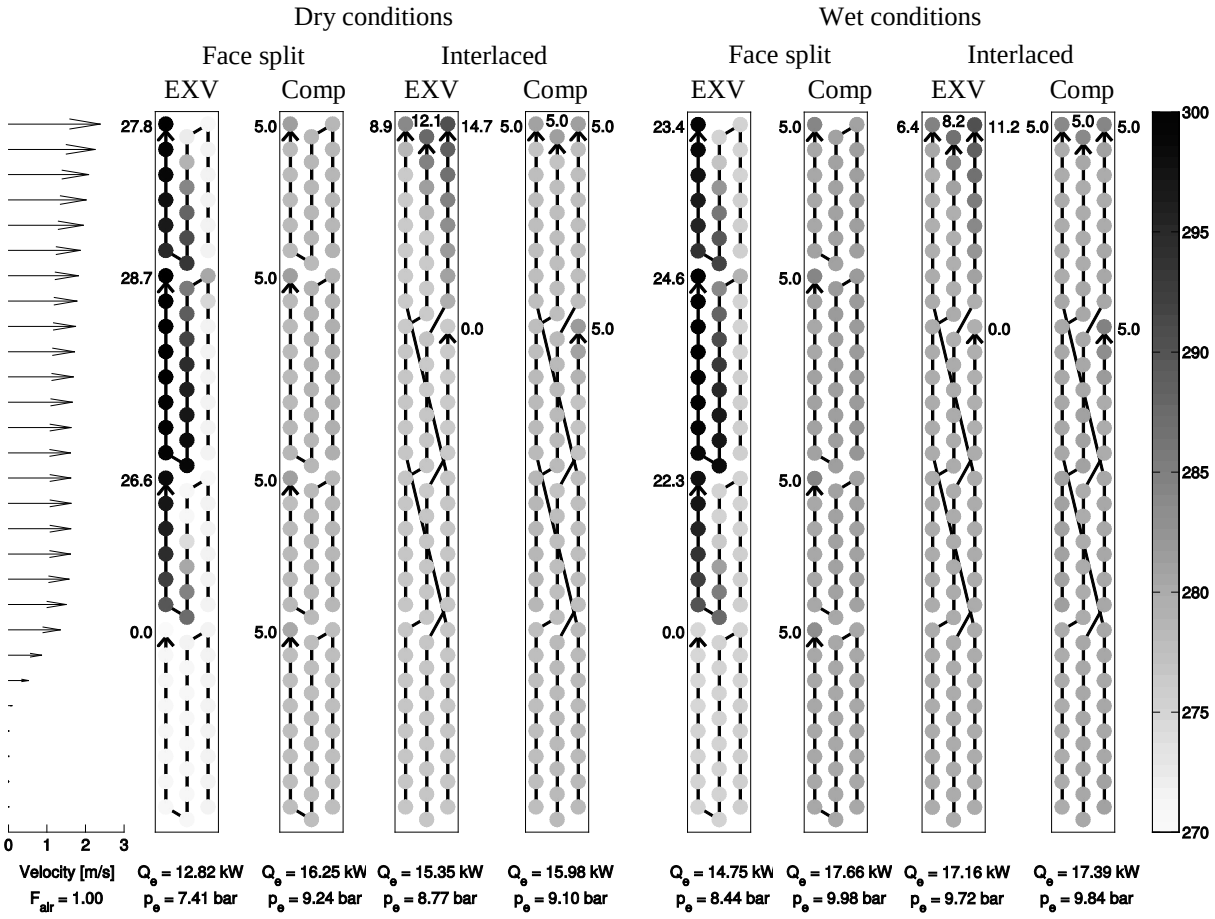

Figure 5: Refrigerant temperature contours and superheats using the CFD predicted air profile

4. DISCUSSION

The benefit in terms of cooling capacity of using the face split evaporator with compensation is not easy measurable. Dry experiments should show differences in cooling capacity, however, wet experiments only give around 3% difference and is below the uncertainty measure in standard experiments (+/- 5%). The simulation results show that the overall UA-value gives a higher percentage improvement by using the compensation method, thus there should be possibilities to minimize the surface area of the evaporator while keeping the same capacity. In order to validate this possibility experimentally, each of the bottom channels in Figure 1b of the face split evaporator were blocked one at a time (both refrigerant and airflow paths). The results of the area blockages are shown in table 4.

Table 4: Possible area savings on face split evaporator with compensation

	No blockage	14% blockage	28% blockage
Cooling capacity (air-side)	15.56 kW	15.33 kW	14.91 kW
Cooling capacity (ref-side)	16.01 kW	15.61 kW	15.34 kW
Mass flow rate	0.0955 kg/s	0.0930 kg/s	0.0907 kg/s
Evaporator outlet pressure	10.73 bar	10.47 bar	10.28 bar
Sensible heat	12.27 kW	12.16 kW	11.93 kW
Latent heat	3.24 kW	3.12 kW	2.93 kW

The experimental results show that the cooling capacity reduces as more area is being blocked, however the degradation is small and below the uncertainty measure. Therefore, the benefits of using the face split evaporator with compensation is revealed and validated by the possible area savings. Note that the simulations in section 3 showed that the overall UA-value improvement were around 7-9% in wet conditions, and thus smaller than what were blocked in the above experiments.

5. CONCLUSION

If airflow maldistribution may be compensated in a way that is independent of circuitry, e.g. by control of individual channel superheats, then the face split circuitry gives the best performance in both dry and wet conditions in general. The capacity gain is slightly lower in wet conditions in general, but below the standard uncertainty in standard experiments for the current design. The percent gain is higher in UA-value, and the benefits of using the compensation method on the face split evaporator were revealed and validated by the possible area savings experimentally. Compared to the interlaced evaporator without compensation, the increase by using the face split evaporator with compensation in wet conditions is around 3% in cooling capacity and 7-9% in UA-value and in dry conditions 7.5% in cooling capacity and 15% in UA-value. It is believed that the compensation method will benefit even more at off-design or part load conditions. Furthermore, we did not take into account other maldistribution sources such as inlet liquid/vapor maldistribution.

REFERENCES

Domanski, P. A., Yashar, D., 2007. Application of an evolution program for refrigerant circuitry optimization. *In Proc. ACRECONF "Challenges To Sustainability"*. New Delhi, India.

Dymola 7.4, 2008. *Dynamic Modeling Laboratory, Dymola User's Manual*, version 7.1. Dynasim AB, Research Park Ideon SE-223 70, Lund, Sweden.

Funder-Kristensen, T., Nicolaisen, H., Holst, J., Rasmussen, M. H., Nissen, J. H., 2009. Refrigeration system. US Patent, Pub. No.: US 2009/0217687 A1.

Jiang, H., 2003. Development of a simulation and optimization tool for heat-exchanger design. Ph.D. thesis, University of Maryland at College Park, Department of Mechanical Engineering.

Kim, J.-H., Braun, J., Groll, E., 2009a. Evaluation of a hybrid method for refrigerant flow balancing in multi-circuit evaporators. *Int. J. Refrigeration* 32, 1283–1292.

Kim, J.-H., Braun, J., Groll, E., 2009b. A hybrid method for refrigerant flow balancing in multi-circuit evaporators: Upstream versus downstream flow control. *Int. J. Refrigeration* 32, 1271–1282.

Kærn, M. R., Brix, W., Elmegaard, B., Larsen, L. F. S., 2011a. Performance of residential air-conditioning systems with flow maldistribution in fin-and-tube evaporators. *Int. J. Refrigeration*, 34 (3), 696 – 706.

Kærn, M. R., Brix, W., Elmegaard, B., Larsen, L. F. S., 2011b. Compensation of flow maldistribution in fin-and-tube evaporators for residential air-conditioning. *Int. J. Refrigeration*, 34 (5), 1230 – 1237.

Kærn, M. R., Elmegaard, B., Larsen, L. F. S., 2011c. Comparison of fin-and-tube interlaced and face split evaporators with flow mal-distribution and compensation. *In Proc. 23th International Congress of Refrigeration*. IIR/IIF, Prague, Czech Republic.

Kærn, M. R., 2011d, Analysis of flow maldistribution in fin-and-tube evaporators for residential air-conditioning systems. PhD thesis, Technical University of Denmark, Kgs. Lyngby, Denmark.

Payne, W. V., Domanski, P. A., 2003. Potential benefits of smart refrigerant distributors. *Air-Conditioning and Refrigeration Technology Institute*, Arlington, VA, USA.

Mader, G., Thybo, C., 2010. An electronic expansion valve with automatic refrigerant distribution control. *In proc. Deutsche Kälte-Klima-Tagung*. Magdeburg, Germany.

Skovrup, M. J., 2010. Thermodynamic and thermophysical properties of refrigerants. Department of Energy Engineering, Technical University of Denmark.

STAR-CD, 2005. *STAR-CD User Guide*, version 3.26. CD-adapco, Melville, NY, USA.